

This article was downloaded by: [Canadian Research Knowledge Network]

On: 13 September 2010

Access details: Access Details: [subscription number 918588849]

Publisher Taylor & Francis

Informa Ltd Registered in England and Wales Registered Number: 1072954 Registered office: Mortimer House, 37-41 Mortimer Street, London W1T 3JH, UK



## Heat Transfer Engineering

Publication details, including instructions for authors and subscription information:

<http://www.informaworld.com/smpp/title~content=t713723051>

### Estimation of Nusselt Number in Microchannels of Arbitrary Cross Section with Constant Axial Heat Flux

Ehsan Sadeghi<sup>a</sup>; Majid Bahrami<sup>b</sup>; Ned Djilali<sup>a</sup>

<sup>a</sup> Department of Mechanical Engineering, University of Victoria, Victoria, British Columbia, Canada <sup>b</sup>

Mechatronic Systems Engineering, School of Engineering Science, Simon Fraser University, Surrey, British Columbia, Canada

Online publication date: 01 February 2010

**To cite this Article** Sadeghi, Ehsan , Bahrami, Majid and Djilali, Ned(2010) 'Estimation of Nusselt Number in Microchannels of Arbitrary Cross Section with Constant Axial Heat Flux', Heat Transfer Engineering, 31: 8, 666 – 674

**To link to this Article:** DOI: 10.1080/01457630903466647

**URL:** <http://dx.doi.org/10.1080/01457630903466647>

PLEASE SCROLL DOWN FOR ARTICLE

Full terms and conditions of use: <http://www.informaworld.com/terms-and-conditions-of-access.pdf>

This article may be used for research, teaching and private study purposes. Any substantial or systematic reproduction, re-distribution, re-selling, loan or sub-licensing, systematic supply or distribution in any form to anyone is expressly forbidden.

The publisher does not give any warranty express or implied or make any representation that the contents will be complete or accurate or up to date. The accuracy of any instructions, formulae and drug doses should be independently verified with primary sources. The publisher shall not be liable for any loss, actions, claims, proceedings, demand or costs or damages whatsoever or howsoever caused arising directly or indirectly in connection with or arising out of the use of this material.

# Estimation of Nusselt Number in Microchannels of Arbitrary Cross Section with Constant Axial Heat Flux

EHSAN SADEGHI,<sup>1</sup> MAJID BAHRAMI,<sup>2</sup> and NED DJILALI<sup>1</sup>

<sup>1</sup>Department of Mechanical Engineering, University of Victoria, Victoria, British Columbia, Canada

<sup>2</sup>Mechatronics Systems Engineering, School of Engineering Science, Simon Fraser University, Surrey, British Columbia, Canada

*In many practical instances such as basic design, parametric study, and optimization analysis of thermal systems, it is often very convenient to have closed form relations to obtain the trends and a reasonable estimate of the Nusselt number. However, finding exact solutions for many practical singly connected cross sections, such as trapezoidal microchannels, is complex. In the present study, the square root of cross-sectional area is proposed as the characteristic length scale for Nusselt number. Using analytical solutions of rectangular, elliptical, and triangular ducts, a compact model for estimation of Nusselt number of fully developed, laminar flow in microchannels of arbitrary cross sections with “H1” boundary condition (constant axial wall heat flux with constant peripheral wall temperature) is developed. The proposed model is only a function of geometrical parameters of the cross section, i.e., area, perimeter, and polar moment of inertia. The present model is verified against analytical and numerical solutions for a wide variety of cross sections with a maximum difference on the order of 9%.*

## INTRODUCTION

Micro-fabrication technologies make it possible to build micro-fluidic, silicon-based microchannels of different cross sections in micro flow devices such as micro-heat sinks, micro-biochips, micro-reactors, and micro-nozzles [1, 2]. It is evident that the understanding of the micro-scale transport phenomena is important for the designer of micro-fluidic devices. For this reason, many studies have been conducted in order to analyze the behavior of the convective flow through microchannels. Reviews of these works have been presented in [3–6].

Using the electrochemical technique to obtain mass transfer coefficients for rectangular microchannels, Acosta et al. [7] showed that the smooth channel correlations for large-sized channels hold for smooth microchannels in laminar and turbulent regimes. Rahman and Gui [8] investigated the laminar

forced convection of water in etched silicon microchannels; they found that the Nusselt numbers were higher than those predicted by analytical solutions for developing laminar flows through rectangular channels.

Shah and London [9] studied heat transfer in ducts for a wide variety of cross-sectional geometries. They reviewed existing studies and calculated Nusselt number for isothermal and isoflux wall conditions numerically.

Muzychka and Yovanovich [10] used the square root of the cross-sectional area of a channel to define the Nusselt number and showed that this length scale is more appropriate than the hydraulic diameter. They proposed two bounds for the Nusselt number of various geometries and developed correlations for these two bounds based on the Fanning friction factor of a rectangular channel.

Duncan and Peterson [4] reviewed micro-scale convective, conduction, and radiation heat transfer. Peng and Wang [11] reported a review of their extensive research on the one-phase and two-phase micro-scale convective heat transfer. Peng et al. [12] analyzed the role of the dimensions of the rectangular microchannels on the Nusselt numbers in laminar and turbulent regimes. They found a strong dependence of the Nusselt number

The authors are grateful for the financial support of the Natural Sciences and Engineering Research Council (NSERC) of Canada, and the Canada Research Chairs Program.

Address correspondence to Ehsan Sadeghi, Department of Mechanical Engineering, University of Victoria, 3800 Finnerty Rd., Victoria, BC, V8W 3P6, Canada. E-mail: ehsans@uvic.ca

on the aspect ratio of the microchannel and proposed some correlations in which the empirical constants are functions of the microchannel dimensions [12]. Bailey et al. [6] concentrated their attention on the single-phase forced convection through microchannels and concluded that the literature is inconclusive with respect to the effect of miniaturization on heat transfer and pressure drop. Many of these studies [4, 6, 11, 12] highlighted that, in many cases, the experimental results for laminar flow through microchannels deviate significantly from the predictions of the conventional theory.

Our literature review indicates that there is no general predictive model for the Nusselt number of an arbitrary cross-section microchannel. Also existing experimental data are inconsistent and sometimes contradictory. For instance, Jiang et al. [13] and Wu et al. [14] reported that in the laminar regime the Nusselt number increases with the Reynolds number with an exponent ranging from 0.3 to 1.96, whereas Gao et al. [15] and Qu et al. [16] showed that in the laminar regime the Nusselt number decreases when the Reynolds number increases.

Analytical, experimental, and numerical models have been developed to predict the Nusselt number in ducts since the 1960s. Several hundred papers on Nusselt number have been published, which illustrates the importance of this topic, and also indicates that the development of a general predictive model is difficult.

In the present study, a compact predictive model is proposed to estimate the Nusselt number for a wide variety of cross-section geometries of channels and microchannels. The proposed model is only a function of geometrical parameters of the cross section, i.e., perimeter, area, and polar moment of inertia.

## PROBLEM STATEMENT

Consider a microchannel with an arbitrary constant cross section as shown in Figure 1. To calculate the Nusselt number, the following assumptions are made:

- Fully developed, steady-state, laminar, and continuum flow.
- Incompressible flow.
- Constant viscosity and thermal conductivity.

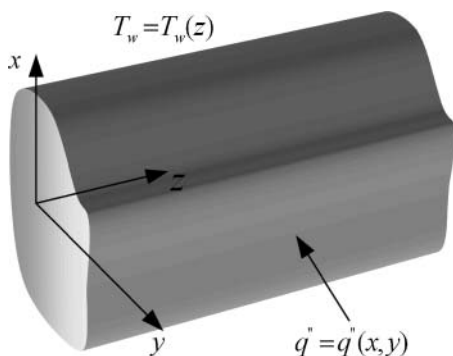


Figure 1 Long Microchannel of arbitrary constant cross section,  $L \gg \sqrt{A}$ .

- Negligible viscous dissipation.
- Negligible rarefaction, slip/jump and surface effects.
- Constant cross-sectional area  $A$  and constant perimeter  $P$ .
- Constant axial wall heat flux with constant peripheral wall temperature (“H1” boundary condition).

Using the preceding assumptions, the energy equation reduces to [9]:

$$\nabla^2 T = \frac{w}{\alpha} \frac{\partial T}{\partial z} \quad \text{with } T = T_w(z) \text{ on the channel wall} \quad (1)$$

Where  $w$  is the axial velocity and  $\alpha$  is the thermal diffusion coefficient of the fluid. The energy balance can be expressed as:

$$q'' \cdot P = \dot{m} c_p (\partial \bar{T} / \partial z) \quad (2)$$

where  $q''$ ,  $c_p$ , and  $\bar{T}$  are wall heat flux, heat capacity, and mean temperature of the  $z$  planes, respectively, and  $\dot{m}$  is the mass flow rate of the fluid, such that  $\dot{m} = \rho \bar{w} A$ . Applying Eq. (2) and introducing the dimensionless parameter  $\theta = (T_w - T) / (q'' \mathcal{L} / k)$ , the energy equation, Eq. (1), after some algebraic manipulations can be simplified to:

$$\nabla^2 \theta = \left( \frac{P}{L A \bar{w}} \right) w, \quad \text{with } \theta = 0 \text{ on the channel wall} \quad (3)$$

where  $P$ ,  $A$ , and  $L$  are the perimeter, the area, and an appropriate characteristic length scale, respectively, and  $\bar{w}$  is the mean axial velocity of the fluid. The Nusselt number based on Eq. (2) can be expressed as:

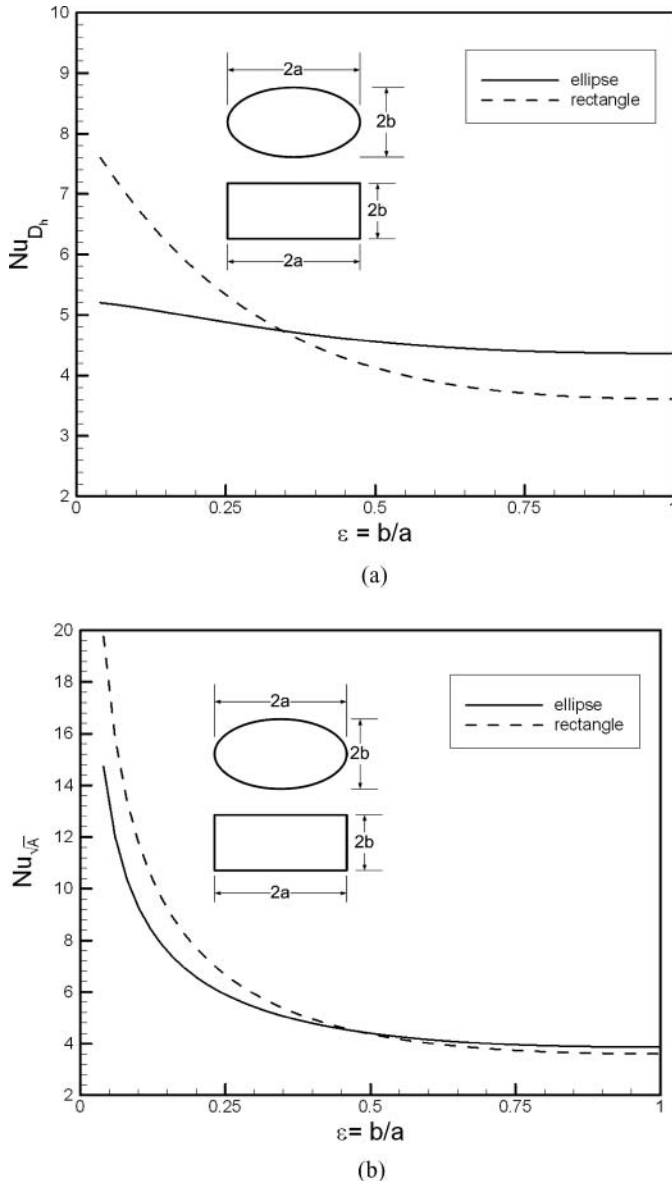
$$Nu_{\mathcal{L}} = \bar{h}_{\mathcal{L}} / k = [q'' / (T_w - \bar{T})] \mathcal{L} / k = 1 / \bar{\theta} \quad (4)$$

where  $\bar{\theta}$  is the area-weighted average dimensionless temperature of the channel cross section. To find the Nusselt number  $\bar{\theta}$  must be calculated by solving Eq. (3). This equation is coupled with the momentum equation. As a result, finding analytical solutions of Eq. (3) for complex geometries of microchannel cross sections is highly unlikely.

## CHARACTERISTIC LENGTH SCALE

To define the Nusselt number, it is conventional to use the ratio of area over perimeter  $D_h = \frac{4A}{P}$ ; i.e., the hydraulic diameter, as the characteristic length scale for noncircular channels. Figure 2 compares the analytical solutions of the “H1” Nusselt number for elliptical and rectangular ducts using hydraulic diameter and square root of cross-sectional area as characteristic length. Elliptical and rectangular cross sections cover a wide range of singly connected microchannels and also these are two bounds of hyperellipse cross sections,  $\left(\frac{x}{a}\right)^n + \left(\frac{y}{b}\right)^n = 1$ , within  $2 \leq n \leq \infty$ . Marco and Han [17] expressed “H1” Nusselt number of rectangular ducts in series form which was correlated by Shah and London [9] within  $\pm 0.03\%$ .

$$Nu_{D_h} = 8.235 [1 - 2.0421\epsilon + 3.0853\epsilon^2 - 2.4765\epsilon^3 + 1.0578\epsilon^4 - 0.1861\epsilon^5] \quad (5)$$



**Figure 2** Comparison between analytical solutions of  $Nu$  for elliptical and rectangular ducts, using (a) hydraulic diameter and (b) square root of area as characteristic length.

where the Nusselt number is based on the hydraulic diameter of the cross section. It can be converted to the Nusselt number based on the square root of area through

$$Nu_{\sqrt{A}} = \frac{P}{4\sqrt{A}} Nu_{D_h} \quad (6)$$

Tyagi [18] found an analytical solution for “H1” Nusselt number of elliptical ducts.

$$Nu_{\sqrt{A}} = \frac{9\pi^2}{E(1-\epsilon^2)\sqrt{\pi\epsilon}} \left\{ \frac{(1+\epsilon^2)[(1+\epsilon^4)+6\epsilon^2]}{17(1+\epsilon^4)+98\epsilon^2} \right\} \quad (7)$$

where  $E(\cdot)$  is the complete elliptic integral of the second kind.

As can be seen in Figure 2, the square root of area,  $\sqrt{A}$ , as the characteristic length scale, leads to more consistent trends

in the solutions of elliptical and rectangular ducts. These shapes cover a wide variety of cross sections; thus, it can be concluded that the square root of area  $\sqrt{A}$  is a more appropriate length scale for Nusselt number, as Muzychka and Yovanovich [10] proposed.

Bahrami et al. [2, 19] showed that the difference between the Poiseuille number,  $f Re_{\sqrt{A}}$ , of elliptical and rectangular ducts is less than 8% over a wide range of aspect ratio. Considering the analogy existing between the Poiseuille number and the Nusselt number [20], similar trends are expected for the Nusselt numbers of these shapes. However, in spite of similar trends, the relative difference between Nusselt numbers of rectangular and elliptical channels is high and reaches up to 35% for small values of aspect ratio ( $\epsilon < 0.1$ ). Thus, developing a general geometric model for the Nusselt number is complicated or impossible. The goal of the present study is to develop a geometric model applicable to several cross sections.

### PROPOSED MODEL

Bahrami et al. [2, 19] developed a compact model for Poiseuille number,  $f Re_{\sqrt{A}}$ , which is only a function of geometrical parameters of the cross section, i.e., perimeter, area, and polar moment of inertia. They started from the analytical solution of elliptical channel and established their model. It was shown that their model is applicable to a wide range of cross sections. Considering the analogy between the Poiseuille number and the Nusselt number [20], the approach proposed by Bahrami et al. [2, 19] is followed to develop a general model for “H1” Nusselt number as a function of geometrical parameters of the cross section.

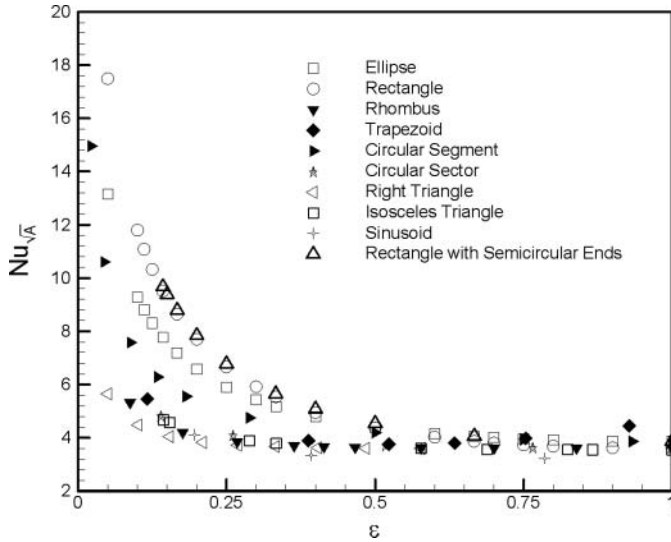
The solution of elliptical channel is selected to develop a general model, not because it is likely to occur more frequently in practice, but rather because of its unique geometrical property of its Nusselt number solution, as in Eq. (7). Applying the definitions of perimeter, area, and polar moment of inertia for elliptical cross section into Eq. (7), the Nusselt number for elliptical ducts can be rewritten as:

$$Nu_{\sqrt{A}} = \left( \frac{144}{17} \pi^2 I_p^* \frac{\sqrt{A}}{P} \right) \frac{\left( \frac{I_p^{*2} + \frac{1}{4\pi^2}}{I_p^{*2} + \frac{4}{17\pi^2}} \right)}{\approx 1} \quad (8)$$

where  $I_p^*$  is dimensionless polar moment of inertia about the center of the cross section,  $I_p/A^2$ . The term in the second set of parentheses in the right-hand side of the preceding equation is approximately equal to unity; therefore, this equation can be simplified to:

$$Nu_{\sqrt{A}} = 8.47 \pi^2 I_p^* \frac{\sqrt{A}}{P} \quad (9)$$

The preceding equation shows that the Nusselt number can be expressed as only a function of geometrical parameters for elliptical ducts. To validate this geometrical function as a general



**Figure 3** Nusselt number for various cross-section geometries versus aspect ratio.

model, the exact values of  $Nu$  for some cross sections are compared with the geometrical function in Eq. (9). A comparison between the analytical solution of rectangular channel and the solution obtained from Eq. (9) shows that:

- i Equation (9) agrees with analytical solution when  $\epsilon > 0.4$ .
- ii For lower aspect ratios, the difference becomes relatively high, 17.1% when  $\epsilon = 0.05$ .
- iii Moreover, when Eq. (9) is applied to other geometries such as rhombus and trapezoid, results are far from analytical or numerical solutions for some aspect ratios and convince us that Eq. (9) is not appropriate to use as a general model.

Figure 3 shows that Nusselt numbers for different geometries are not in agreement. However, two bounds can be recognized for Nusselt numbers, where the upper bound is provided by elliptical and rectangular cross sections and the lower bound is presented by triangular cross sections. Thus, different cross sections can be categorized into three groups: (1) cross sections close to rectangle/ellipse, (2) cross sections close to triangle, and (3) cross sections close to both of the previous groups.

Equation (9) shows the Nusselt number as a function of  $I_p^*$ ,  $\frac{\sqrt{A}}{P}$ , for elliptical ducts. It implies that if there is a general model for various geometries, it can be a function of  $I_p^*$ ,  $\frac{\sqrt{A}}{P}$ . Thus, a new model is proposed as a product function of geometric parameters of the cross section, i.e., dimensionless polar moment of inertia  $I_p^*$ , and square root of area over perimeter,  $\frac{\sqrt{A}}{P}$ .

$$Nu_{\sqrt{A}} = c_1 (I_p^*)^{c_2} \left( \frac{\sqrt{A}}{P} \right)^{c_3} \quad (10)$$

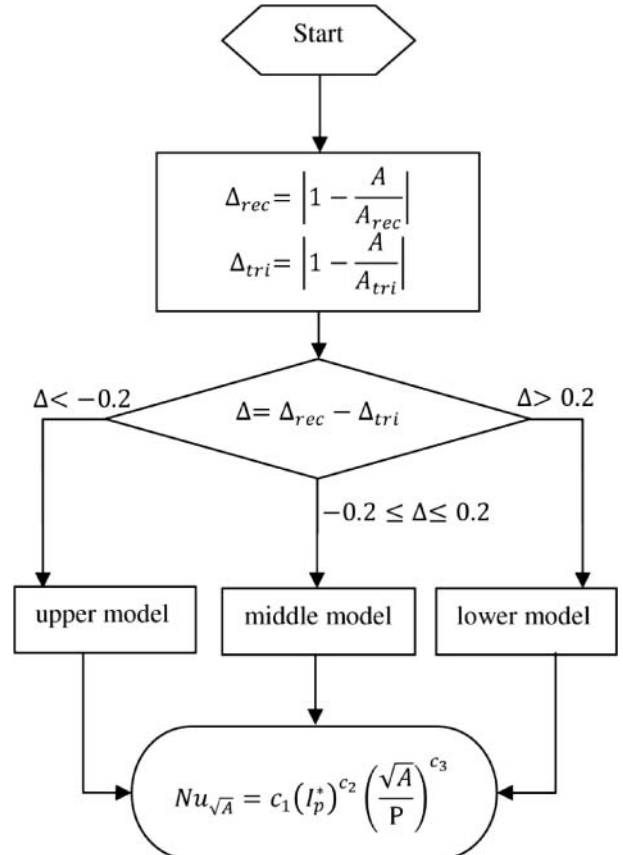
The proposed model, Eq. (10), consists of three submodels: upper, lower, and middle. Coefficients  $c_1$ ,  $c_2$ , and  $c_3$  are determined by minimizing differences between Eq. (10) and analytical so-

**Table 1** Coefficients of the proposed model

Model	Coefficient		
	$c_1$	$c_2$	$c_3$
Upper	108.84	1.04	1.09
Lower	7.91	0.38	0.15
Middle	$\frac{\text{upper model} + \text{lower model}}{2}$		

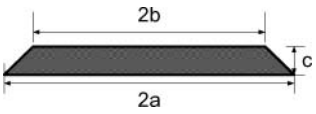
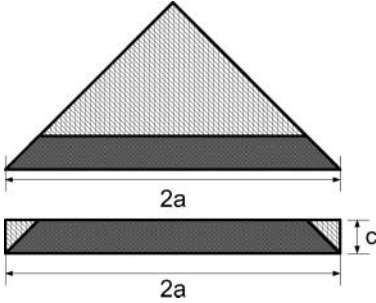

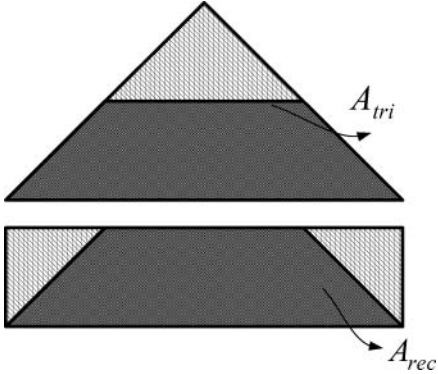
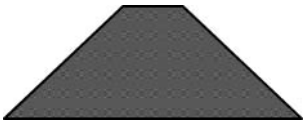
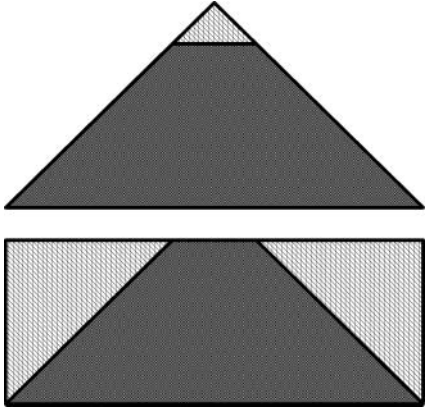
lutions of elliptical and rectangular ducts for the upper model, and that of right triangular and isosceles triangular ducts for the lower model. The middle model is defined as the average of the upper and the lower models. Coefficients  $c_1$ ,  $c_2$ , and  $c_3$  are listed in Table 1 for the proposed model.

To apply the model, first we should find out which submodel is appropriate to use. Relative deviation of the channel cross-sectional area from rectangular and triangular shapes is proposed as a measure to select the proper submodel. The reference rectangular and triangular cross section is defined based on the limiting cases of geometry. These limiting cases generally occur in bounds of aspect ratios or shape angles. For instance, as shown in Table 2, the trapezoid yields rectangle when the aspect ratio goes to zero and/or  $\phi$  goes to 90 and approaches the triangle when the aspect ratio becomes higher and the upper base goes to zero. Figure 4 illustrates the procedure to apply the model.



**Figure 4** Flowchart for applying the proposed model.

**Table 2** Limiting cases for trapezoidal cross section

Cross section	Limiting cases	Appropriate submodel
		Upper
		Middle
		Lower

### VALIDATION OF THE MODEL

In this section, the present model is compared with numerical results of Shah and London [9] for various cross sections. Equation (5) is used to convert the reported Nusselt number in the literature from  $D_h$  base to  $\sqrt{A}$  base. Geometrical parameters required for evaluating the Nusselt number are reported for various geometries in Table 3.

#### *Elliptical and Rectangular Channels*

Elliptical and rectangular cross sections are bases for developing the upper model. Rectangular cross section can be manufactured by photolithographic-based processes such as Si

chemical etching and has various engineering applications [5]. Figure 5 shows the comparison between numerical results [9] and the model for elliptical and rectangular cross sections. The difference between the present model and numerical results is less than 8% for these shapes.

#### *Triangular Channels*

The lower model is developed based on the solutions of different types of triangular cross sections. Figure 6 shows the comparison between numerical results [9, 21] and the model. The maximum difference between the present model and numerical results is 6.6%.

**Table 3** Geometric parameters of studied cross sections

Cross section	aspect ratio	$\frac{\sqrt{A}}{P}$	$I_p^*$
	$\epsilon = \frac{b}{a}$	$\frac{\sqrt{\pi\epsilon}}{4E(1-\epsilon^2)}$	$\frac{1+\epsilon^2}{4\pi\epsilon}$
	$\epsilon = \frac{b}{a}$	$\frac{\sqrt{\epsilon}}{2(1+\epsilon)}$	$\frac{1+\epsilon^2}{12\epsilon}$
	$\epsilon = \frac{b}{a}$	$\frac{\sqrt{2\epsilon}}{2(1+\frac{1}{\sin\phi})}$	$\frac{\epsilon}{9} + \frac{1}{12\epsilon}$
	$\epsilon = \frac{b}{a}$	$\frac{\sqrt{2\epsilon}}{2(1+\epsilon+\sqrt{1+\epsilon^2})}$	$\frac{1}{9}(\epsilon + \frac{7}{9\epsilon})$
	$\epsilon = \frac{c}{a+b}$	$\frac{1}{2(\frac{1}{\epsilon} + \frac{1}{\sin\phi})\sqrt{\epsilon}}$	$\frac{2(\epsilon^2+3)+\beta^{(1)}(\epsilon^2-3)}{36\epsilon}$
	$\epsilon = \frac{b}{a}$	$\frac{\sqrt{\sin\phi}}{4}$	$\frac{1}{6\sin\phi}$
	$\epsilon = 1$	$\frac{1}{2\sqrt{n}\tan(\frac{\pi}{n})}$	$\frac{1}{6n} \left( \tan\left(\frac{\pi}{n}\right) + \frac{3}{\tan\left(\frac{\pi}{n}\right)} \right)$
	$\epsilon = \frac{b}{a}$	$\frac{\sqrt{4\epsilon(1-\epsilon)+\pi\epsilon^2}}{2(2-2\epsilon+\pi\epsilon)}$	$\frac{f^{(2)}}{(4\epsilon(1-\epsilon)+\pi\epsilon^2)^2}$
	$\epsilon = \frac{b}{a}$	$\frac{\sqrt{2\epsilon}}{2+\frac{2}{\pi}E(-\pi^2\epsilon^2)}$	$\frac{1}{12\epsilon} \left( 2 - \frac{12}{\pi^2} + 5\epsilon^2 \right) - \frac{9\epsilon}{32}$

(1)  $\beta = 1 - \frac{\epsilon^2}{\tan\phi^2}$  (2)  $f = \left[ \frac{4\epsilon(1-\epsilon)[\epsilon^2+(1-\epsilon)^2]}{3} + 2\epsilon^2 \left( \frac{\pi}{4} - \frac{8}{9\pi} \right) + \pi\epsilon^2 \left( 1 - \epsilon + \frac{4\epsilon}{3\pi} \right)^2 \right]$

**Trapezoidal Channel**

Trapezoidal cross section is an important geometry since some microchannels are manufactured with trapezoidal cross sections as a result of the etching process in silicon wafers [5]. Furthermore, in the limit when the top side length goes

to zero, it yields an isosceles triangle. At the other limit when top and bottom sides are equal, it becomes rectangle/square [2]. Figure 7 shows the comparison between the approximate model and the numerical data reported by [9] for different values of  $\phi$ . As can be seen, except for a few points, the agreement between the model and the numerical values is reasonable (less than 8%).

Downloaded By: [Canadian Research Knowledge Network] At: 23:46 13 September 2010

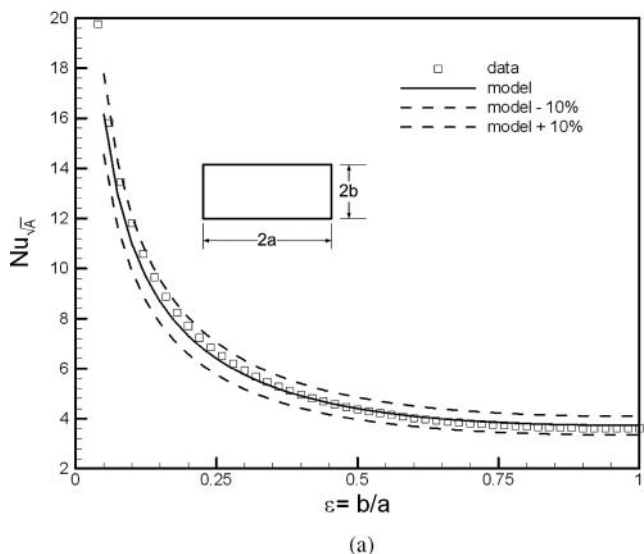
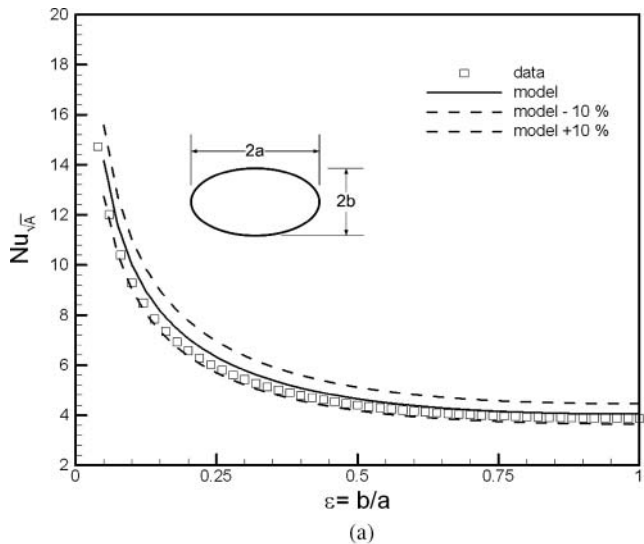


Figure 5 Comparison of present model and numerical values [9] for (a) elliptical channel and (b) rectangular channel.

Table 4 Comparison of present model and numerical values [9] for rhombic channel

$\phi$	$\epsilon$	Data	Model	Percent difference
10	0.087	5.318	5.547	4.13
20	0.176	4.201	4.511	6.87
30	0.268	3.849	4.018	4.19
40	0.364	3.703	3.721	0.49
45	0.414	3.663	3.615	-1.33
50	0.466	3.642	3.528	-3.26
60	0.577	3.618	3.398	-6.48
70	0.700	3.610	3.314	-8.93
80	0.839	3.609	3.511	-2.78
90	1	3.608	3.489	-3.41

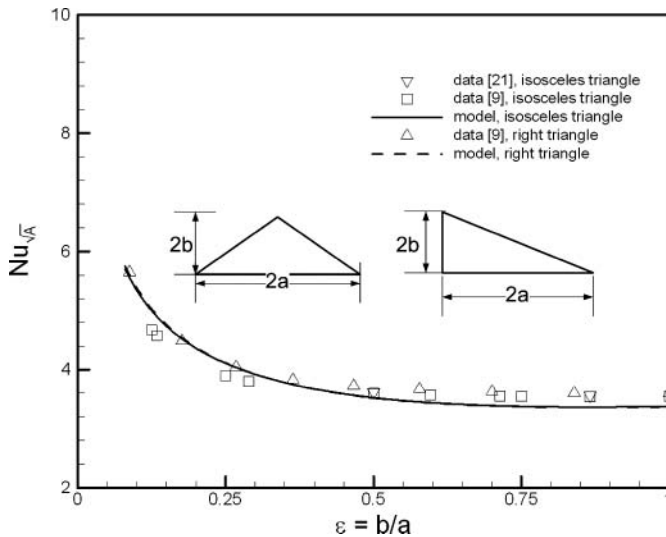


Figure 6 Comparison of present model and numerical values [9, 21] for isosceles and right-angle triangular channels.

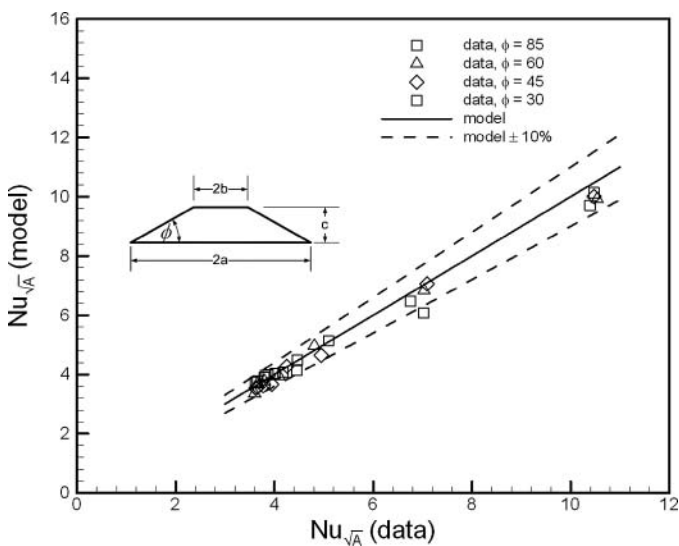
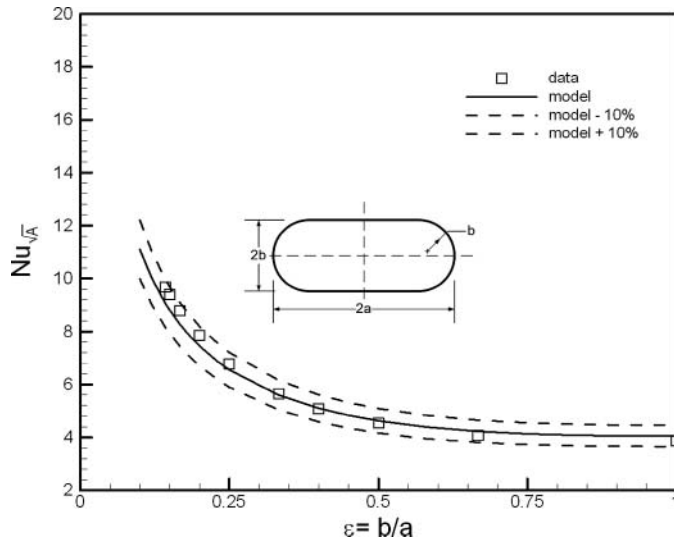


Figure 7 Comparison of present model and numerical values [9] for trapezoidal channel.

Table 5 Comparison of present model and numerical values [9] for regular polygonal channel

$n$	Data	Model	Percent difference
3	3.546	3.368	-5.27
4	3.608	3.726	3.17
5	3.678	3.809	3.46
6	3.724	3.872	3.81
7	3.766	3.915	3.81
8	3.780	3.945	4.18
9	3.797	3.966	4.26
10	3.809	3.982	4.32
20	3.852	4.033	4.49
$\infty$	3.867	4.051	4.54





**Figure 8** Comparison of present model and numerical values [9] for rectangular channel with semicircular ends.

### Other Cross Sections

The present model is also compared with numerical results for a number of geometries listed in Table 3. The results are shown in Tables 1 and 2 and Figures 8 and 9.

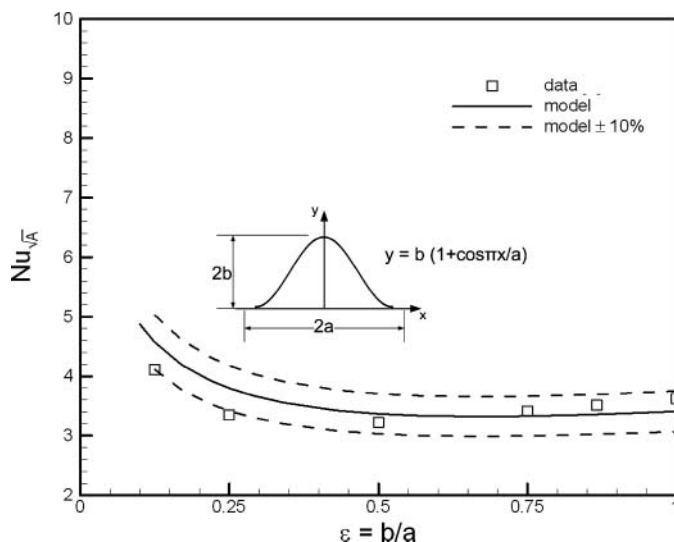
### CONCLUSIONS

In this article, closed-form relations have been developed for the Nusselt number of fully developed laminar flow in smooth arbitrary cross sections channels with “H1” boundary condition (constant axial wall heat flux with constant peripheral wall temperature). The square root of area,  $\sqrt{A}$ , is adopted as the characteristic length scale, as it is superior to the conventional

hydraulic diameter,  $D_h$ . Using existing analytical solutions for temperature distribution in elliptical, rectangular, and triangular ducts, a compact model including three sub-models (upper, lower, and middle models) has been developed. The present model is only a function of geometrical parameters of the cross section, i.e., area, perimeter, and polar moment of inertia. The proposed model was compared with numerical results for channels with cross sections including ellipse, rectangle, triangle, trapezoid, rhombus, regular polygon, rectangle with semicircular ends, and sine, and was found to successfully predicts the Nusselt number for a wide variety of shapes with a maximum difference on the order of 10%.

### NOMENCLATURE

$A$	cross-sectional area, $m^2$
$A_{rec}$	area of limiting rectangle of a cross section, $m^2$
$A_{tri}$	area of limiting triangle of a cross section
$c_1, c_2, c_3$	coefficients used in Eq. (10)
$c_p$	heat capacity at constant pressure, $kJ/kg\cdot K$
$D_h$	hydraulic diameter, $m$
$E(\cdot)$	complete elliptic integral of the second kind
$fRe$	Poiseuille number
$\bar{h}$	thermal convection coefficient, $W/m^2\cdot K$
$I_p$	polar moment of inertia, $m^4$
$I_p^*$	dimensionless polar moment of inertia
$\mathcal{L}$	side of a rhombic cross section, $m$
$\mathcal{L}$	characteristic length scale, $m$
$Nu$	Nusselt number
$n$	number of sides of a polygon
$P$	perimeter, $m$
$q''$	heat flux, $W/m^2$
$T$	temperature, $K$
$\bar{T}$	mean temperature, $K$
$T_w$	wall temperature, $K$
$\bar{T}_w$	mean wall temperature, $K$
$w$	velocity in $z$ -direction, $m/s$



**Figure 9** Comparison of present model and numerical values [9] for sine channel.

### REFERENCES

- [1] Yang, C., Wu, J., Chien, H., and Lu, S., Friction Characteristics of Water, R-134a, and Air in Small Tubes, *Microscale Thermophysical Engineering*, vol. 7, pp. 335–348, 2003.
- [2] Bahrami, M., Yovanovich, M. M., and Culham, J. R., Pressure Drop of Laminar, Fully Developed Flow in Microchannels of Arbitrary Cross-Section, *ASME Journal of Fluid Engineering*, vol. 126, pp. 1036–1044, 2006.
- [3] Obot, N. T., Toward a Better Understanding of Friction and Heat/Mass Transfer in Microchannels—A Literature Review, *Journal of Nanoscale and Microscale Thermophysical Engineering*, vol. 6, pp. 155–173, 2002.
- [4] Duncan, A. B., and Peterson, G. P., Review of Microscale Heat Transfer, *ASME Applied Mechanics Review*, vol. 47, pp. 397–428, 1994.

- [5] Morini, G. L., Single-Phase Convective Heat Transfer in Microchannels: A Review of Experimental Results, *International Journal of Thermal Sciences*, vol. 43, pp. 631–651, 2004.
- [6] Bailey, D. K., Ameen, T. A., Warrington, R. O., and Savoie, T. I., Single Phase Forced Convection Heat Transfer in Microgeometries—A Review, *Proc. IECEC Conference ASME-FL*, Orlando, FL, ES-396, 1995.
- [7] Acosta, R. E., Muller, R. H., and Tobias, W.C., Transport Processes in Narrow (Capillary) Channels, *AIChE Journal*, vol. 31, pp. 473–482, 1985.
- [8] Rahman, M. M., and Gui, F. J., Experimental Measurements of Fluid Flow and Heat Transfer in Microchannel Cooling Passages in a Chip Substrate, *Advances in Electronic Packaging, ASME EEP*, vol. 199, pp. 685–692, 1993.
- [9] Shah, R. K., and London, A. L., *Laminar Flow Forced Convection in Ducts*, Academic Press, New York, 1978.
- [10] Muzychka, Y. S., and Yovanovich, M. M., Laminar Flow Friction and Heat Transfer in Non-Circular Ducts and Channels: Part II—Thermal Problem, *Proc. Compact Heat Exchangers, A Festschrift on the 60th Birthday of Ramesh K. Shah*, Grenoble, France, pp. 131–139, 2002.
- [11] Peng, X. F., and Wang, B. X., Forced Convection and Boiling Characteristics in Microchannels, *Proc. 11th Int. Heat Transfer Conference*, Kyongyu, Korea, vol. 1, pp. 371–390, 1998.
- [12] Peng, X. F., Peterson, G. P., and Wang, B. X., Frictional Flow Characteristics of Water Flowing Through Rectangular Microchannels, *Journal of Experimental Heat Transfer*, vol. 7, pp. 249–264, 1995.
- [13] Jiang, P. X., Fan, M. H., Si, G. S., and Ren, Z. P., Thermal-Hydraulic Performance of Small Scale Micro-Channel and Porous-Media Heat Exchangers, *International Journal of Heat and Mass Transfer*, vol. 44, pp. 1039–1051, 2001.
- [14] Wu, H. Y., and Cheng, P., An Experimental Study of Convective Heat Transfer in Silicon Microchannels with Different Surface Conditions, *International Journal of Heat and Mass Transfer*, vol. 46, pp. 2547–2556, 2003.
- [15] Gao, P., Le Person, S., and Favre-Marinet, M., Scale Effects on Hydrodynamics and Heat Transfer in Two-Dimensional Mini and Microchannels, *International Journal of Thermal Science*, vol. 41, pp. 1017–1027, 2002.
- [16] Qu, W., Mala, G. M., and Li, D., Heat Transfer for Water Flow in Trapezoidal Silicon Microchannels, *International Journal of Heat and Mass Transfer*, vol. 43, pp. 3925–3936, 2000.
- [17] Marco, S. M., and Han, L. S., A Note on Limiting Laminar Nusselt Number in Ducts with Constant Temperature Gradient by Analogy to Thin-Plate Theory, *Trans. ASME*, vol. 77, pp. 625–630, 1955.
- [18] Tyagi, V. P., Laminar Forced Convection of a Dissipative Fluid in a Channel, *Journal of Heat Transfer*, vol. 88, pp. 161–169, 1966.
- [19] Bahrami, M., Yovanovich, M. M., and Culham, J. R., A Novel Solution for Pressure Drop in Singly Connected Microchannels of Arbitrary Cross-Section, *International Journal of Heat and Mass Transfer*, vol. 50, pp. 2492–2502, 2007.
- [20] Incropera, F. P., and DeWitt, D. P., *Fundamentals of Heat and Mass Transfer*, 4th ed., John Wiley & Sons, New York, 1996.
- [21] Chen, S., Chan, T. L., Leung, C. W., and Yu, B., Numerical Prediction of Laminar Forced Convection in Triangular Ducts with Unstructured Triangular Grid Method, *Journal of Numerical Heat Transfer*, vol. 38, pp. 209–224, 2000.



**Ehsan Sadeghi** is a Ph.D. candidate in the department of mechanical engineering at University of Victoria, BC, Canada. Also, he is a member of the institute for integrated energy systems (IESVic). His research mostly focuses on the analytical and experimental investigations of transport phenomena in high-porosity materials including metal foams and gas diffusion layers used in fuel cells. Other research interests are contact resistance, image analysis, heat transfer in microscale, and advanced numerical simulations.



**Majid Bahrami** is an assistant professor with the School of Engineering at the Simon Fraser University, BC, Canada. Research interests include modeling and characterization of transport phenomena in microchannels and metal foams, contacting surfaces and thermal interfaces, development of compact analytical and empirical models at micro- and nano-scale, and microelectronics cooling. He has numerous publications in refereed journals and conferences. He is a member of ASME, AIAA, and CSME.



**Ned Djilali** is professor of mechanical engineering and holds the Canada Research Chair in Energy Systems Design and Computational Modeling at the University of Victoria, where he also served as director of the Institute for Integrated Energy Systems (IESVic) for several years. His current research interests focus on thermofluid science, transport phenomena, renewable energy systems integration, and fuel cell technology. He lectures widely on sustainable energy issues, holds several research awards and four patents, is the

author of more than 200 papers, and collaborates and consults with leading fuel cell developers.